BEST: Journal of Recent Trends in Social Sciences
Research & Development (BEST: JRTSSRD)
Vol. 1, Issue 1, Jun 2016, 27-36

STUDY OF ALUMINUM DOPED ZNO THIN FILMS DEPOSITED ON GLASS SUBSTRATE FOR AN APPLICATION OF H_2 AND NH_3 GASES SENSING

RASHID HASHIM JABBAR

Center of Applied Physics, Ministry of Higher Education and Scientific Research, Baghdad, Iraq

ABSTRACT

This paper presents the structural properties of ZnO and ZnO: Al (2, 4, 6 and 8)%. nano structurethin films deposited at 450 ^{o}C on glass substrates by chemical spray pyrolysis in thichness (150±5 nm). The structure of ZnO and ZnO: Al is nano-structure films were found to exhibit as hexagonal wurtzite structure. The structural details and microstructure were obtained from X-ray diffraction shows that the increase of Aluminum concentration caused to decrease the grain size, interplaner spacing. The surface Morphology of the films was studied by using the Scanning Electron Microscopy (SEM), Atomic Force Microscopy (AFM), and the Transmission electron microscopy (TEM), sensitivity of films increases with the increase of Al concentration and substrate temperature.

KEYWORDS: Zno: Alnanostructures, Aluminum Doped, And Structural Properties

INTRODUCTION

Transparent conducting oxides (TCOs) are a special class of materials that can simultaneously be both optically transparent and electrically conducting and, as such, are acritical component in almost all thin-film photovoltaic devices. TCOs are generally based ona limited class of metal oxide semiconductors such In2O3, ZnO and SnO2, which aretransparent due to their large band gap and can also tolerate very high electronic doping concentrations to yield conductivities of 1000 S/cm or higher. Semiconductor ZnO is the subject of research for a lot of applications for the past several years, because the material is bio safe, chemically stable, biocompatible and nontoxic. ZnO has a band gap of around 3.2-3.37eV at R.T. [1, 2]. It has strong of ionic and exciton binding energy of 60 meV [3]. ZnO has low resistivity and high transparency in the visible range and high light trapping characteristics [3, 4]. ZnO has attracted increasing attention as a potential material for devices of optoelectronic such as low threshold blue UV lasers, solar cells, LEDs, sensors, display devices and photodetectors [5-7]. In recent years, it has been found that ZnO can be synthesized by various routes such as electron beam evaporation technique [5], chemical spray pyrolysis technique [1], RF thermal plasmaevaporation [6], sol gel method [3, 7], and precipitation methods[1, 7]. Among these methods, precipitation has many advantages over the other methods, for example, it is unsophisticated and a low cost method [2, 4, 8]. Zinc oxide (ZnO) has been used in a wide range of products for many years, including, among others, varistors, surface acoustic wave devices and cosmetics. Besides these established applications, ZnO and its ternary alloys are now also being considered as potential materials for optoelectronic applications, such as light emitting diodes, photovoltaic, sensors, displays, etc[9].

EXPERIMENTAL

Nanostructure films of ZnO, ZnO: Alprepared by spray pyrolysis deposition (SPD) technique in air from zinc nitrate [(Zn $(NO_3)_2.6H_2O$)- 99.9% purity, molecular weight (297.4 g/mole))], and using aluminum nitrate [(Al

$(NO_3)_3.9H_2O$) 99.9% purity, molecular weight: 375.13 g/mol.]. Diluted with distilled water to concentration of molarities equal 0.075 M. The deposition method involves the decomposition of an aqueous solution of zinc nitrate. The spray solution is sprayed onto heated substrates held at 450°C. The time of the deposition is 3 sec. each 42 sec., Compressed air is used as a gas carrier and it is fed with the solution into a spray nozzle at a readjusted constant atomization pressure. Film thickness (***t***=150±5 nm). Diffraction studies are carried out using X- Ray with filtered CuKα radiation 0.15406 nm wavelengths) was performed to identify the crystalline phases present in the deposited films.

RESULTS AND DISCUSSIONS

Structural Analysis

The XRD graphs of ZnO and ZnO: Alnanostructure films are shown in figure 1. It is obvious the nanostructure film is polycrystalline for ZnO, ZnO:Al 2% and amorphous for ZnO:Al 6% and ZnO:Al 8%, which is an indication of lattice Shrinkage [10]. Planes 100 and 101 are grown with aluminum doping concentration of 2% and 4% thin disappear for more Al concentration, beside the growth of 002 plane is exhibit for ZnO pure.

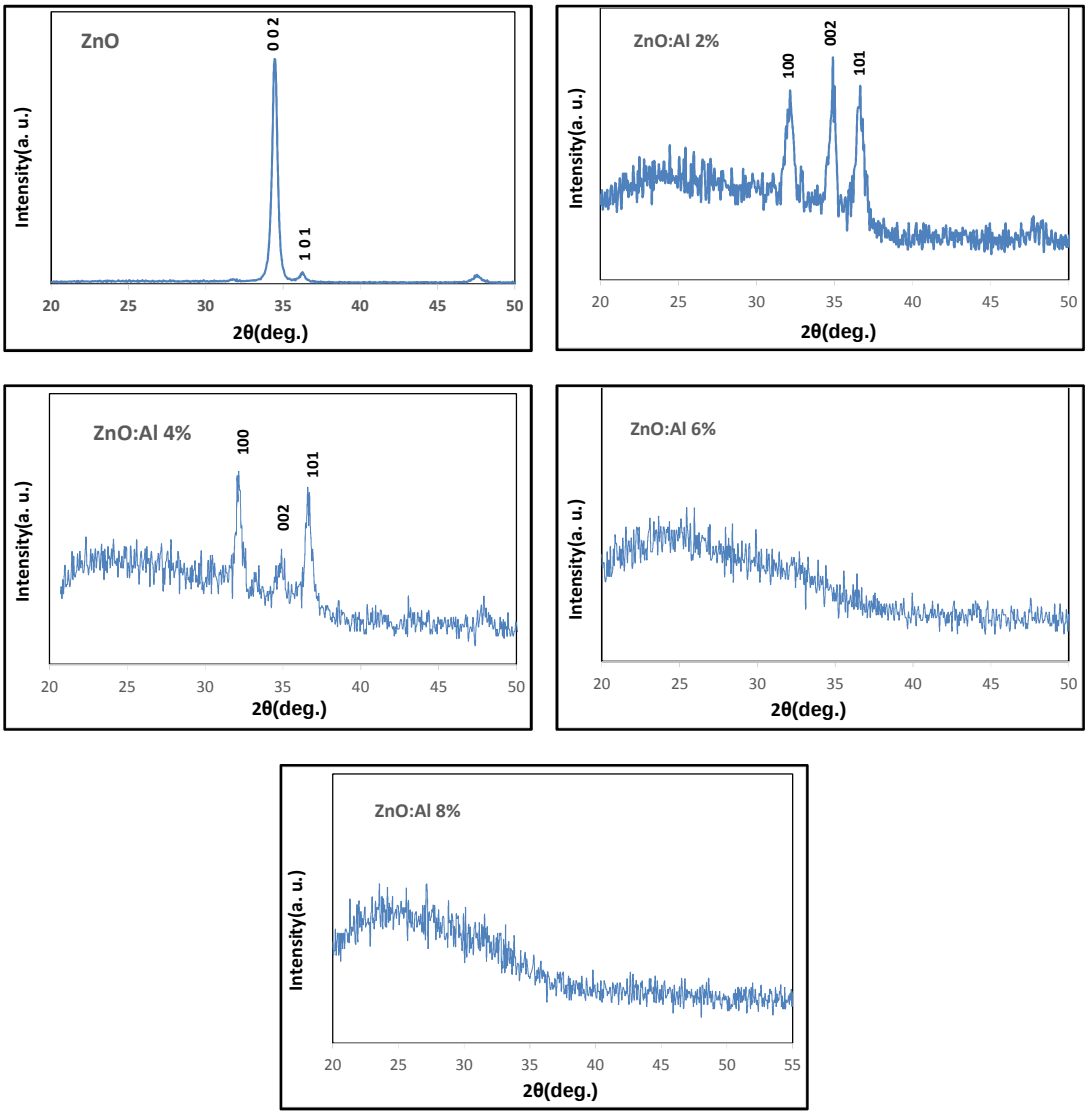

Figure 1: X-Ray Diffraction Pattern of Zno And Zno: Al Nanostructure with Concentration (2, 4, 6 And 8) %

The values which measured by XRD instrument of diffraction angle(2θ), Inter planer spacing(d) and Full Width at Half Maximum (FWHM) are in table (1). The lattice parameters $\boldsymbol{a}$ and $\boldsymbol{c}$ were calculated from the XRD pattern using the equation [11, 12].

$$\frac{1}{d^2} = \frac{4}{3}\left[\frac{h^2+hk+k^2}{a^2}\right] + \frac{l^2}{c^2} \quad (9)$$

The micro strain ($\boldsymbol{\varepsilon}$) can be calculated from the relation [13]:

$$\varepsilon = \left[\frac{|C_{ASTM} - C_{XRD}|}{C_{ASTM}}\right] \times 100\% \quad (10)$$

According to the values in table (1), the interplanner spacing(d) is decreases with the increases of aluminum doping due to the ion size of the Al^{3+} (r= 0.054 nm) interstitial in Zn^{2+} (r= 0.074 nm) [14].

Table 1: XRD Patterns, Lattice Parameter *d* Spacing, *FWHM* and Micro Strain For Zno and Zno: Al Nanostructure Films Deposited Atsubstrate Temperature 450 ^oC on Glass Substrates

Hkl	Doping (%)	2θ(deg.)	D(nm)	A(nm)	C(nm)	Micro Strain	FWHM(Deg.)
100	0	-	-				-
	2	32.1224	2.78424	0.32150	0.51508	0.0107	0.4219
	4	32.1617	2.78093	0.32111	0.51447	0.0119	0.4295
002	0	34.4751	2.59943	0.32450	0.51989	0.0015	0.3961
	2	34.8989	2.56883	0.32068	0.51377	0.0132	0.4219
	4	34.8463	0.256259	0.31990	0.51252	0.0156	0.5167
101	0	36.2462	2.47637	0.32505	0.52077	0.0002	0.3938
	2	36.6198	2.45196	0.32184	0.51564	0.0097	0.5667
	4	36.6393	2.4507	0.32168	0.51537	0.0102	0.4442

The averagecrystallet size D_g was calculated by Scherer equation [15]:

$$D_g = \frac{k\lambda}{\beta cos\,(\theta)} \quad (1)$$

Where λ is the wave length of incident X-ray radiation , β is the intrinsic full width at Half Maximum of the peak , and θ is the Bragg's diffraction angle of the respective XRD peak .Assumes the world Warren that the mathematical representation of curves resulting from the XRD depends primarily on the amount of similarity between these curves and functions of each of the Cauchy and Gauss, in the case considered curve X-ray diffraction is similar to function Cauchy and take the form of $\frac{1}{\sqrt{1+k^2x^2}}$, the correction is given by the following relationship, which was called (Scherer's correction):

$$\beta_{cs} = \beta_m - \beta_i \quad (2)$$

Where β_m:is the measured full width at Half Maximum of the peak, β_i: is the instrumental broadening [16], where $(\beta_i) = 0.11\ deg.$ for the used instrument. Compensation equation (2) in the relationship (1) we get:

$$D_g = \frac{k\lambda}{(\beta_m - \beta_i)\cos(\theta)} \quad (3)$$

In the case considered XRD curve similar to the function Gauss which takes the form ($e^{-k^2x^2}$) theaccuracy to be higher because of the great similarity between this function and the diffraction curves; it was suggested (Warren correction) form:

$$\beta_{cs}{}^2 = \beta_m{}^2 - \beta_i{}^2 \quad (4)$$

This correction called (Warren's Correction). Compensation equation (4) in the relationship (1) we get:

$$D_g = \frac{k\lambda}{\sqrt{\beta_m{}^2 - \beta_i{}^2}\cos(\theta)} \quad (5)$$

Since the output line shape does not resemble the Gauss curve and Cauchy curve completely, so these relations have limited operation values. If the intensity curve does not sharp may be used (Scherer's correction) or (Warren's Correction) former because the difference between the values given by relations (3) and (5) is not large, which means that the decrease of the curve breadth means that the effect of the amount (β_i) is significant,since the width of the curve in the half intensity (FWHM) is inversely proportional with crystallite size according to equation (1), the decrease in (FWHM) leads to increase in the crystallite size, which means that few crystal defects are present in the sample. Moreover, Warren was suggested a relationship takes into account the geometric meaning which is [17, 18]:

$$\beta_{cs} = \sqrt{(\beta_m - \beta_i)\sqrt{(\beta_m{}^2 - \beta_i{}^2)}} \quad (6)$$

Compensation equation (6) in the relationship (1) we get:

$$D_g = \frac{k\lambda}{\sqrt{(\beta_m - \beta_i)\sqrt{(\beta_m{}^2 - \beta_i{}^2)}\cos(\theta)}} \quad (7)$$

The crystallite size of (100),(002) and (101) planes using equations (1,3,5 and 7), where the crystallets decreases with the increase of Aluminum doping concentration as shown is in table (2).

Table 2: The Crystallet Size for 100, 002 And 101 Plane of Zno, Zno: Alnanostructure Films

Hkℓ	Doping (%)	Crystallet Size (nm)				Dislocation Density (σ) ($\times 10^{11}$ Lines/cm^2)
		eq.(1)	eq.(3)	eq.(5)	eq.(7)	
100	0					
	2	20.5	27.7	21.2	24.2	1.70
	4	20.1	27.0	20.8	23.7	1.78
002	0	21.9	30.4	22.8	26.3	1.44
	2	20.6	27.9	21.4	24.4	1.68
	4	16.8	21.4	17.2	19.2	2.71
101	0	22.2	30.8	23.1	26.7	1.41
	2	15.4	19.1	15.7	17.4	3.32
	4	13.6	16.4	13.8	15.0	4.43

The dislocation density(σ) which represents the defect in the film was determined from the formula [11]:

$$\sigma = \frac{1}{D_g{}^2} \quad (8)$$

- **Surface Morphology**

TEM shows the mean size of the grains more than XRD. This difference in the size refers to this fact that “TEM shows the size of the particles and XRD shows the size of the crystallites” [19]. The presence of ZnO spherical nanoparticles along with a few nanorods was observed as shown in figure (2). The grain sizes of spherical particles were

found to be in the range of (6.5–23 nm). This results and TEM images of ZnO the thin film pattern agree with [20, 21].

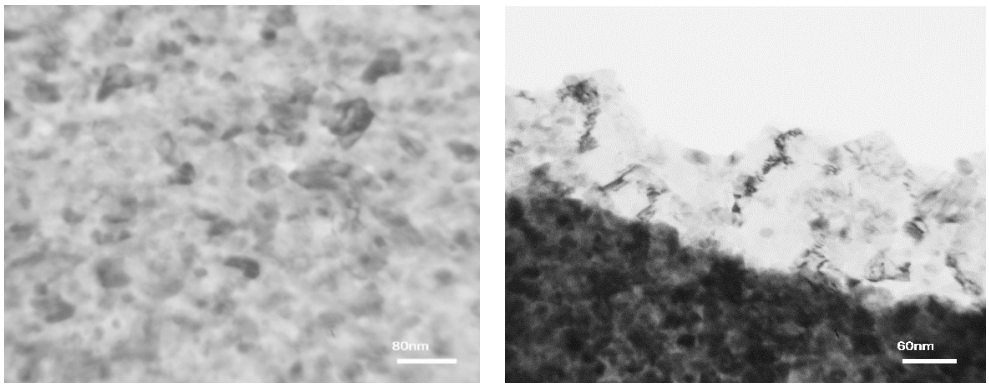

Figure 2: TEM Image of Undoped Zno

Using scanning electron microscope (SEM) as shown in figure (3). The change in the morphology of ZnO, ZnO:Al nanostructure films is due to the difference in ionic radius between $Al^{3+}$and Zn^{2+} [14].The pictures of morphological structure of the films were obtained by using an atomic force microscopy are shown in Figure (4).

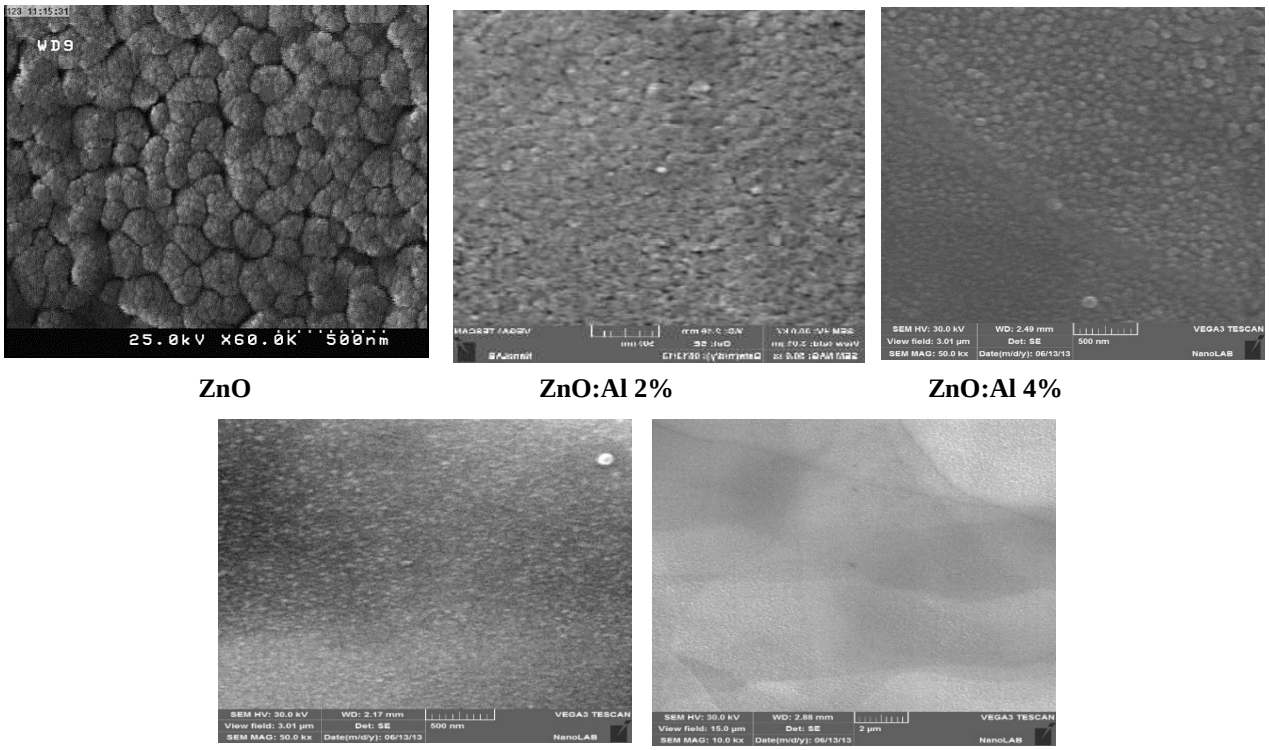

ZnO **ZnO:Al 2%** **ZnO:Al 4%**

ZnO:Al 6% **ZnO:Al 8%**

Figure 3: SEM image of ZnO anZnO:B Nanostructure thin Films with Doping Concentration (2, 4, 6 and 8)%

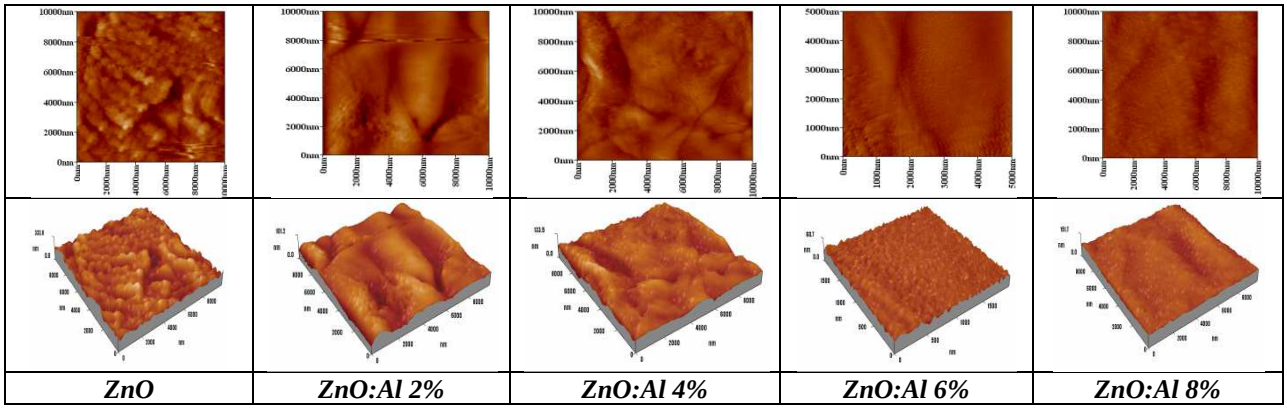

Figure 4: Morphological of The Zno and Zno:B Nanostructures With Concentration (2, 4, 6 And 8) %. an Atomic Force Microscopy (AFM)

AFM and SEM images of ZnO and ZnO:Al thin films deposited on glass substrate shows that the grain size decreased and the roughness increase with the increase of Aluminum ratio due to crystal distortion caused by the Al concentrations, values of the grain size and roughness measured by AFM and SEM are shown in the table (3).

Table 3: Grain Size Calculated by AFM, SEM and Roughness Average of Zno and Zno:Al Thin Films Deposited on Glass Substrate

sample	DAFM-PS (nm)	DSEM-PS (nm)	Sa(Roughness Average)(nm)
ZnO	31.4	29.2	6.8
ZnO:B 2%	28.7	23.5	8.6
ZnO:B 4%	25.1	19.7	9.1
ZnO:B 6%	19.3	16.2	10.3
ZnO:B 8%	16.8	12.5	11.5

Sensing Properties of H_2 Gas

The sensing mechanism of ZnO towards H_2 gas depends on the interaction between the reducing gas and the negatively charged O^{2-} ions on the ZnO thin films surface, thereby causing a variation in conductance, as described by equation [22]:

$$H_2(ad) \rightarrow 2H^+ + 2e^- \quad (2)$$

So that, by the electrons released back into the ZnO conduction band and increasing the carrier doped in the ZnO active layer, the resistance of the sensor is decreased upon exposure to a reducing gas [23]. Figure (5, a) shows sensitivity for ZnO, ZnO:Al nanostructure thin films as a function of operating time for H_2 gas with concentration (50ppm) at R.T.[23].Figures (5, b) shows the sensitivity of films vs. substrate temperature, in general the sensitivity increases with increasing of substrate.

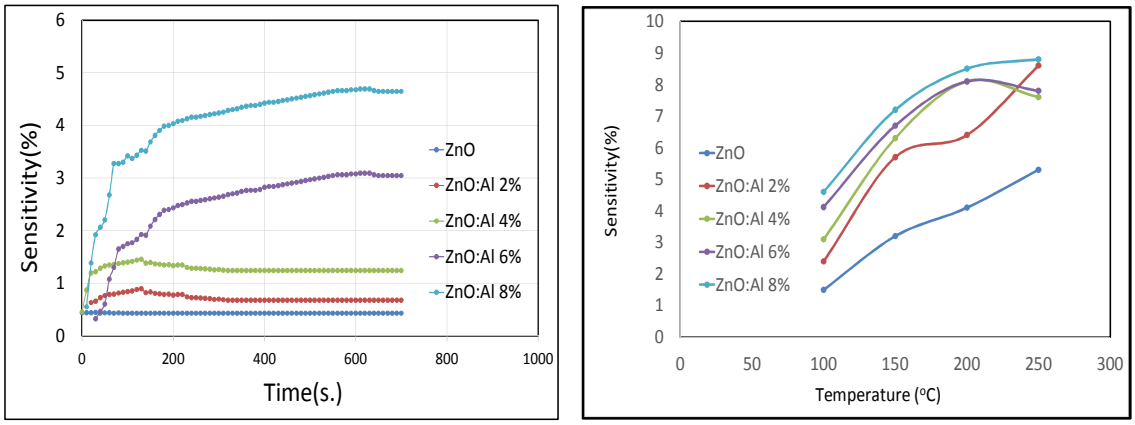

(a) **(b)**

Figure 5: Sensitivity For Zno, Zno:Al With Doping Concentration (2, 4, 6 And 8)%. Deposited on Glass Substrateas a Function of Operating Time for H_2gas With Concentration 50 Ppm for Substrate Temp,(A) At R.T., (B) 100-250 ^{O}c.

Sensing Properties of NH_3 Gas

It is known that the sensing mechanism of ZnO towards NH_3 gas depends on the interaction between thereducing gas and the negatively charged O^{2-} ions on the ZnO thin films surface, thereby causing a variation in conductance, as described by equation [24]:

$$2NH_3 + 3O^{2-} \rightarrow 3H_2O + N_2 + 3e^- \quad (4\text{-}3)$$

So that, by the electrons released back into the ZnO conduction band and increasing the carrier doped in the ZnO active layer, the resistance of the sensor is decreased upon exposure to a reducing gas [25]. Figure (6, a) shows the sensitivity of ZnO and ZnO:Al as function of operating time for NH_3 gas at room temperature with concentration (50ppm) at R.T. prepared at 450 ^{o}C. Figure(6, b) shows the sensitivity of films vs. substrate temperature, as shown in the figure the sensitivity increase with increasing temperature until reach to highest sensitivity at 150^{o}C then decrease above this temperature, also the sensitivity increase with increasing of aluminum-boron co-doped concentration.

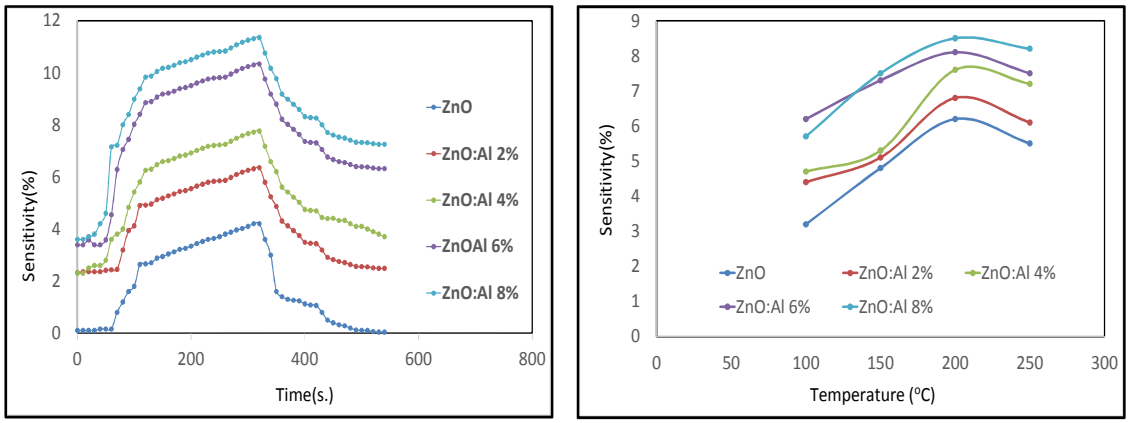

(a) **(b)**

Figure 6: Sensitivity For Zno, Zno: Al With Doping Concentration (2, 4, 6 And 8) %. Deposited on Glasssubstrate as a Function of Operating Time for NH_3 Gas With Concentration 50 Ppm for Substrate Temperature, (A) At R.T., (B) 100-250 Oc

CONCLUSIONS

It was found that the increase of concentration of Aluminum due to decrease of grain size in general and varying the morphology, 100, 002 and 101 planes has disappear in 6% and 8% doping concentration, the lattice constants decreases with the increase of doping. ZnO and ZnO: Alnanostructures have been synthesized on glass substrate using a low cost spray pyrolysis deposition. The average roughness of the films increased with the doped concentrations so that the thin films sensitivity increases. Increase of substrate temperature leads to increase of sensitivity of the films.

REFERENCES

1. T. V. VIMALKUMAR," Highly conductive and transparent ZnO thin film using Chemical Spray Pyrolysis technique: Effect of doping and deposition parameters ", Doctor of Philosophy Thesis, COCHIN University Of Science And Technology, August 2011.
2. Ersin Kayahan," White light luminescence from annealed thin ZnO deposited porous silicon", Journal of Luminescence, 130 (2010) 1295–1299
3. Svetlana Spitsina,"Growth, Doping, and Characterization of ZnO Nanowires: Application in a Miniaturized Gas Ionization Sensor", phd. Thesis In the Department of Electrical and Computer Engineering, Concordia University, Canada, (2013)
4. D. Gültekin, M. Alaf and H. Akbulut,"Synthesis and Characterization of ZnONanopowders and ZnO-CNT NanocompositesPrepared by Chemical Precipitation Route", Vol. 123 (2013).
5. V. K. Dwivedi, P. Srivastava, and G. Vijaya Prakash," Photoconductivity and surface chemical analysis of ZnO thin films deposited by solution-processing techniques for nano and microstructure fabrication", Vol. 34, No. 3 Journal of Semiconductors March 2013
6. Josef W. Spalenka, Padma Gopalan, Howard E. Katz, and Paul G. Evans," Electron mobility enhancement in ZnO thin films via surface modification bycarboxylic acids APPLIED PHYSICS LETTERS 102, 041602 (2013).
7. T.O. Berestok, D.I. Kurbatov, N.M. Opanasyuk, A.D. Pogrebnjak1,"Structural Properties of ZnO Thin Films Obtained by Chemical Bath Deposition Technique, JOURNAL OF NANO- AND ELECTRONIC PHYSICS, Vol. 5 No 1, 01009(4pp) (2013)
8. Mohit Agarwal, Pankaj Modi, R.O. Dusane," Study of Electrical, Optical and Structural Properties of Al- Doped ZnO Thin Filmson PEN Substrates" JOURNAL OF NANO- AND ELECTRONIC PHYSICS, Vol. 5 No 2, 02027(4pp) (2013)
9. Firoz Khan, Abdul Mobin, M. Husain," Formation of ZnO by Annealing of Thermally Evaporated Zinc in Oxygen Ambient for Solar Cell Application", ISSN- 2277-1956.
10. A.V. Singh, "Al-doped zinc oxide (ZnO:Al) thin films by pulsed laser ablation", Indian Institute of Science. 81, pp. 527-533, 2001.
11. Hassan Wahab, "Metal oxide catalysts for carbon nanotubes growth**:** The growth mechanism using NiO and doped ZnO", phd. Thesis Department of Electronic, University of York, (2012).

12. Mareike Trunk, "Novel ZnO-based Ternary Oxides for Optoelectronic Applications", phd. Thesis, Department of Physics, University of Oslo, (2012).
13. T. Obata , K. Komeda , T. Nakao , H. Ueba , and C. Tasygama , J. Appl. Phys. , 81 , (1997) , 199 .
14. V. Kumar , R.G. Singh, Neetu Singh, Avinashi Kapoor , R.M. Mehra , L.P. Purohit," Synthesis and characterization of aluminum–boron co-doped ZnO nanostructures", Materials Research Bulletin, Vol. 48, pp. 362–366, 2013.
15. James R. Connolly, "Elementary Crystallography for X-Ray Diffraction" EPS400-002, (2012)
16. S MONDAL, S R BHATTACHARYYA and P MITRA, "Effect of Al doping on microstructure and optical band gapof ZnO thin film synthesized by successive ion layer adsorption and reaction", PRAMANA journal of physics, Indian Academy of Sciences Vol. 80, No. 2,—February (2013) pp. 315–326
17. L.V. Azarooff. (1968). Mc Graw-Hill Book Company. 552-556.
18. R. Romero, M.C. López, D. Leinen, F. Mart´ın, J.R. Ramos Barrado, "Materials Science and Engineering ", Vol. 110, pp. 87–93, 2004.
19. Th.H.DE.Keijser. (1982). J. Appl. Cryst., 15, 308-314.
20. E. Comini, G. Faglia, M. Ferroni, A. Ponzoni, A. Vomiero, G. Sberveglieri, "Metal oxide nanowires: Preparation and application in gas sensing", J. Mol. Catal. A-Chem., Vol. 305, pp. 170-177, 2009.
21. P. Mitra and A.K. Mukhopadhyay," ZnO thin film as methane sensor", Vol. 55, No. 3, pp. 281-285 2007.
22. D. Aswal, S. Gupta, "Science and technology of chemiresistor gas sensors", in, Nova Science Publishers, 2007.
23. J. B. K, Law and J. T. L. Thong, "Improving the NH3 gas sensitivity of ZnO nanowire sensors by reducing the carrier concentration", Nanotechnology, Vol. 19, 205502 (5pp), 2008.
24. S. Park and Jung-Hyuk Kohm," Electrical and optical properties of in and al doped ZnO thin film", Electronic Materials Letters, Vol. 9, No. 4, pp. 493-496, 2013.
25. J. B. K, Law and J. T. L. Thong, "Improving the NH3 gas sensitivity of ZnO nanowire sensors by reducing the carrier concentration", Nanotechnology, Vol. 19, 205502 (5pp), 2008.
26. N. Le Hung, "Synthesis and Gas Sensing Properties of ZnO Nanostructures", Journal of the Korean Physical Society, Vol. 57, No. 6, pp. 1784-1788, 2010.